Electronic Supplementary Material (ESI) for Journal of Materials Chemistry C.

A SERS sensor based on 3D nanocone forests capable of intelligent classification of aquatic product dyes

Yaqian Zhao[a,b], Ruoyang Huang[a,b], Xin Li[a,b], Xuanjiao Mao[b,c], Shaohang Xu[a,b], Na Zhou[a,b], Shaojuan Li[b,d,*], Haiyang Mao[a,b,*], Chengjun Huang[a,b]

[a] *Institute of Microelectronics of Chinese Academy of Sciences, Beijing 100029, P. R. China*

[b] *University of Chinese Academy of Sciences, Beijing 100049, P. R. China*

[c] *The People's Hospital of Pingyang, Wenzhou 325499, P. R. China.*

[d] *State Key Laboratory of Applied Optics, Changchun Institute of Optics Fine Mechanics and Physics, Chinese Academy of Sciences, Changchun 130033, P. R. China.*

Corresponding authors: maohaiyang@ime.ac.cn; lishaojuan@ciomp.ac.cn

We use a two-step etching process to prepare the NCFs. A large area of NWFs are obtained by the first step of plasma etching with O_2 or Ar. In the second etching process, NWFs act as masks to obtain composite nanostructures. Finally, residual NWFs are removed by wet etching with BHF acid to obtain NCFs.

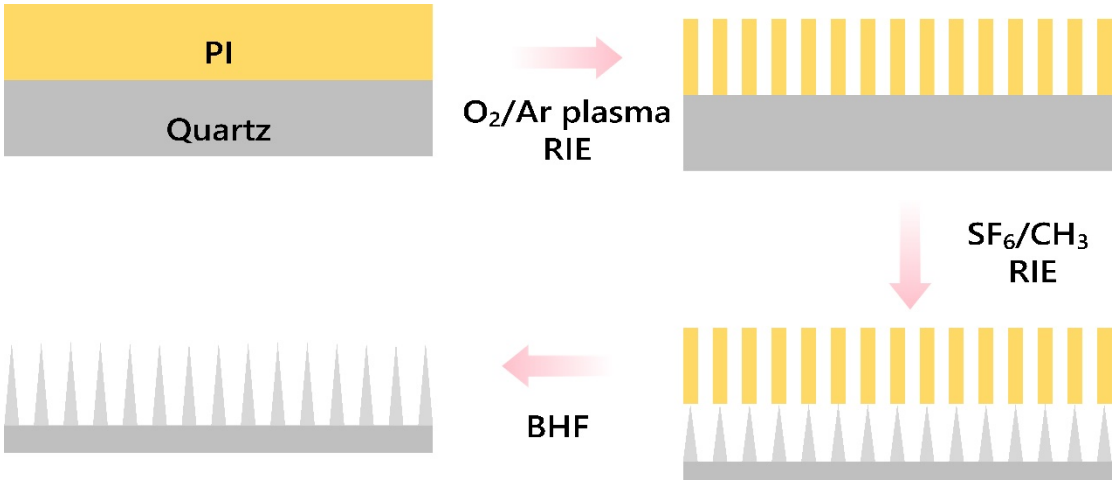

Figure S1. Fabrication process of nanocone forests

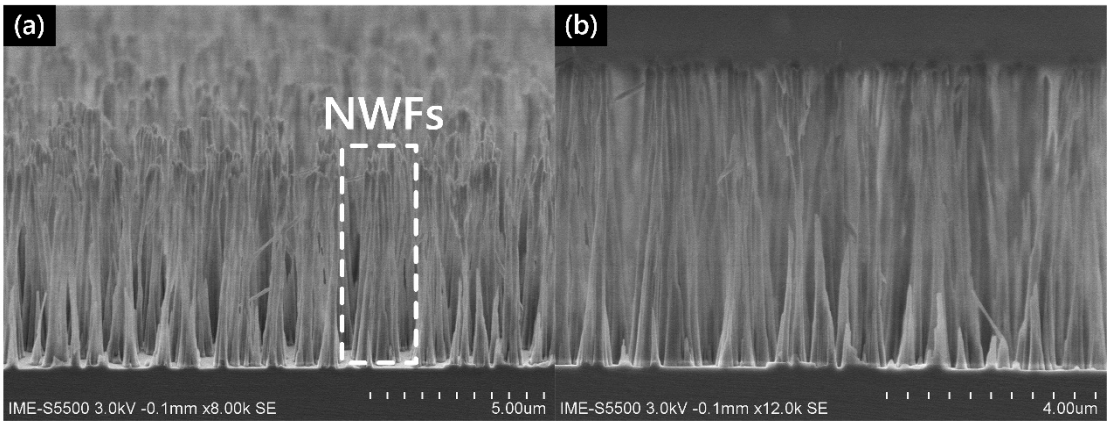

Figure S2. A SEM image of the NWFs

The composite nanostructures composed of NWFs and NCFs were obtained after the two-step etching process. The composite nanostructures have two layers. The preferred NWFs are located in the upper layer, and the NCFs are located directly below the NWFs.

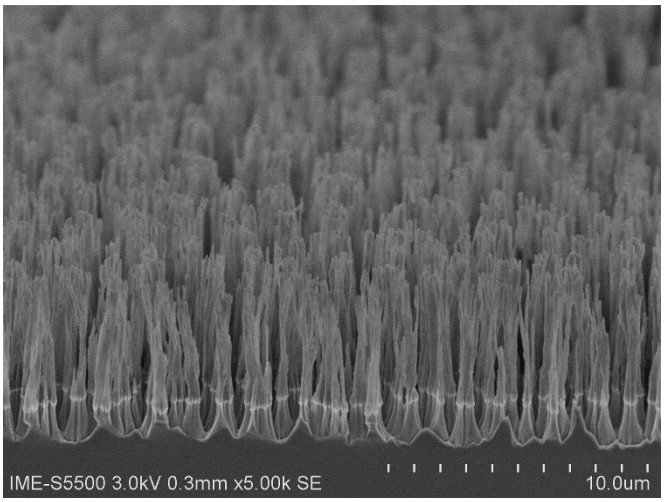

Figure S3. Nanocone forests with nanowire forests standing on their tops

To obtain uniformly distributed AuNPs on the flat silicon surface, we investigated the effect of pH value of buffer solution on the result of AuNPs fixation. In all experiments, the concentration of AuNPs was 0.5mg/ml. Affected by electrostatic interaction, negatively charged AuNPs can be deposited on positively charged P4VP templates. When the pH value of the buffer solution is close to pKa, AuNPs can be closely distributed on the flat silicon surface. If the pH value is further reduced, it will cause two-dimensional accumulation of AuNPs and thus affect the distribution of AuNPs.

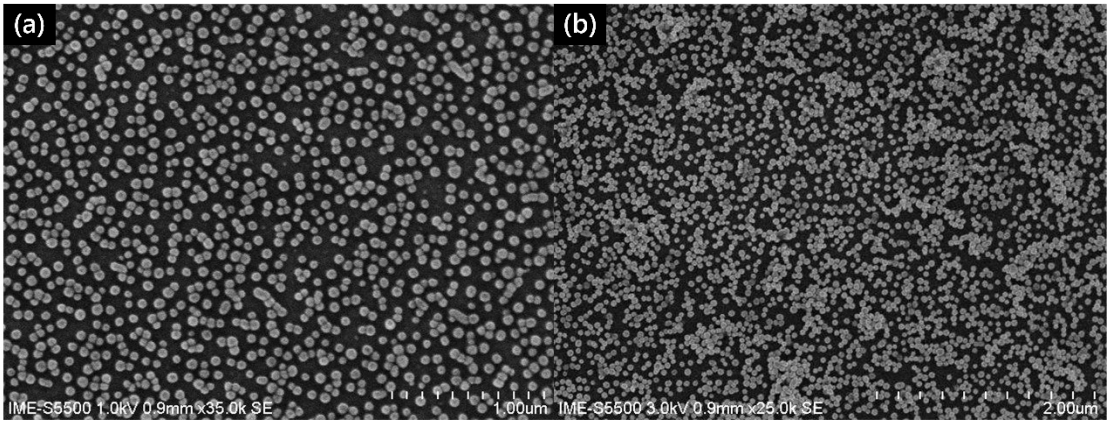

Figure S4. Distribution of AuNPs on the substrate using varying pH values, (a) 4.5, and (b) 3.5.

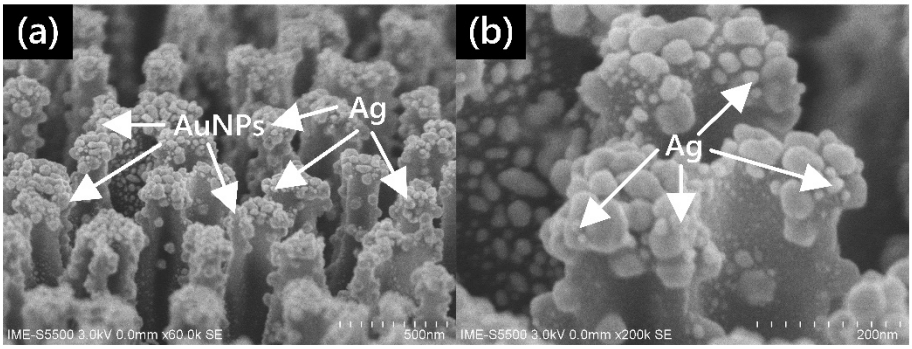

Figure S5 (a) SEM image of another location of the 3D Ag-AuNPs@NCFs structure, (b) Partial enlarged image of (a)

Table S1. Primary SERS peaks and corresponding vibration modes of R6G molecules.

SERS peak (cm^{-1})	**Vibration mode**
612	C-C-C ring bending in-plane
1184	C-H in-plane bending
1311	N-H in plane bending
1361, 1513, 1649	Aromatic C-C stretching

In order to calculate the EF of the 3D Ag-AuNPs@NCF-based sensor, we obtained the SERS spectra of 10^{-8} M R6G solution measured by the sensor and 10^{-2} M R6G solution measured on a flat silicon. The EF of the sensor at different Raman peaks are obtained by analyzing different Raman peak intensities.

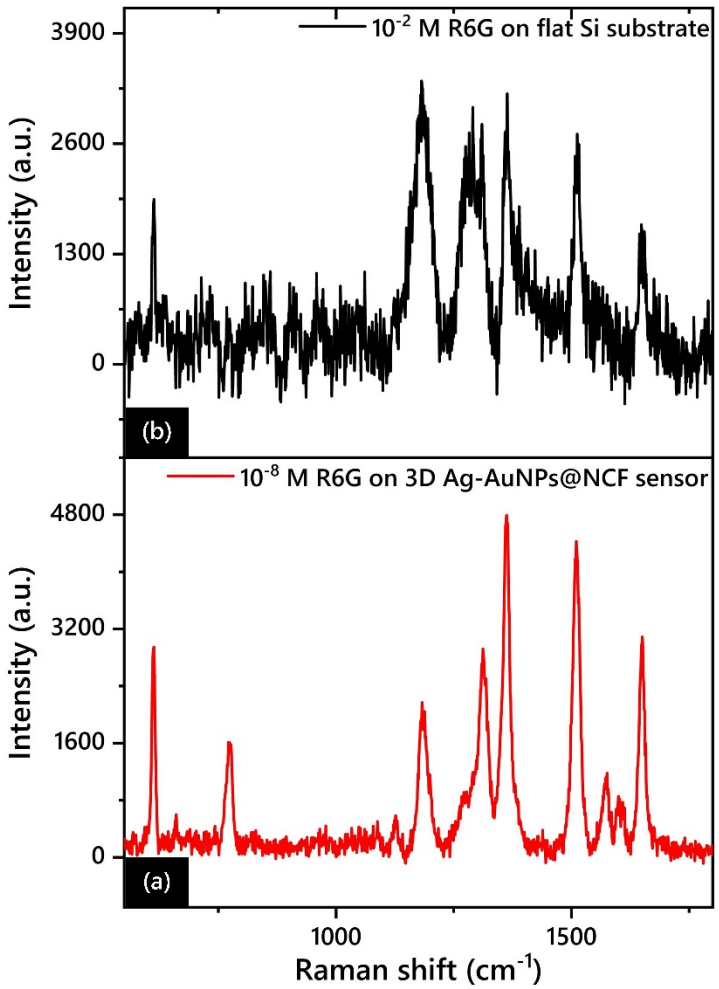

Figure S6. SERS spectra of (a) 10^{-8} M detected on the 3D Ag-AuNPs@NCF sensor, and (b) 10^{-2} M R6G detected on a flat Si substrate.

According to the measured spectra, we calculated the Raman intensities of the four main characteristic peaks in the table and also the ratio of I_{SERS}/I_{REF}. For the convenience of calculation, we used the concentration of R6G solution to approximate the number of R6G molecules mentioned in the EF calculation formula. The calculation results show that the maximum EF of the sensor is 1.89×10^6.

Table. S2 The I_{SERS}/I_{REF} ratios of the 3D Ag-AuNPs@NCF sensor at the four characteristic peaks of 612 cm^{-1}, 1184 cm^{-1}, 1361 cm^{-1}, and 1649 cm^{-1}, respectively.

Raman shift (cm^{-1})	**612**	**1184**	**1361**	**1649**
I_{SERS} (a.u.)	2946.47534	1787.10449	4688.57422	2990.6709
I_{REF} (a.u.)	1945.2019	2738.08643	2753.89502	1583.1554
I_{SERS}/I_{REF}	1.51	0.65	1.7	1.89

We evaluated the repeatability of the 3D Ag-AuNPs@NCF-based sensor by calculating the RSD of different Raman peaks. We tested the SERS spectra of 10^{-7} M R6G solution at 20 different locations using the 3D Ag-AuNPs@NCF-based sensor, and calculated the RSD values of 612, 1184, 1361 and 1649 cm^{-1} as 6.48%, 5.80%, 5.93% and 6.46%, respectively. The results show that the RSD of the sensor is less than 6.48% and has excellent repeatability.

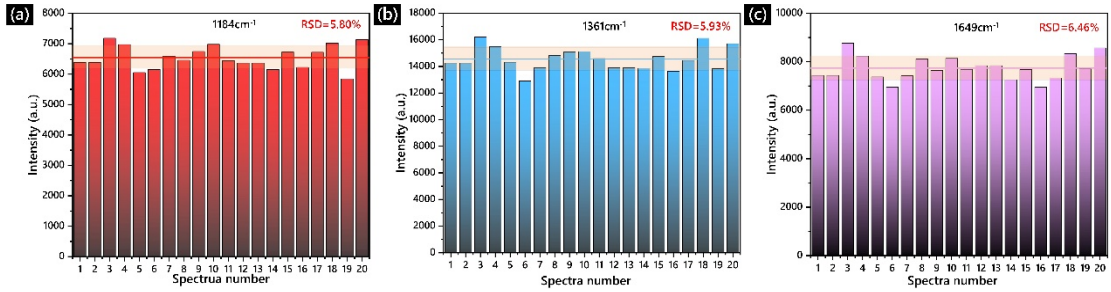

Figure S7. The SERS intensities of characteristic peaks at (a) 1184 cm^{-1}, (b)1361 cm^{-1}, and (c) 1649 cm^{-1}, acquired from the Raman spectra of 10^{-7} M R6G.

We prepared five SERS sensors using the same method and performed signal coherence analysis of different batches of sensors using spectra measured with 10-7M R6G solution. During the test, three spectra were randomly acquired for each sensor, and the signal intensity at the 612 cm-1 characteristic peak was selected in each spectrum for calculation and analysis. The signal intensities of the spectra obtained from different SERS sensors ranged from 8500-10000, and the RSDs of the sensors 1-5 were 6.71%, 6.42%, 7.15%, 5.9% and 7.31%, respectively.

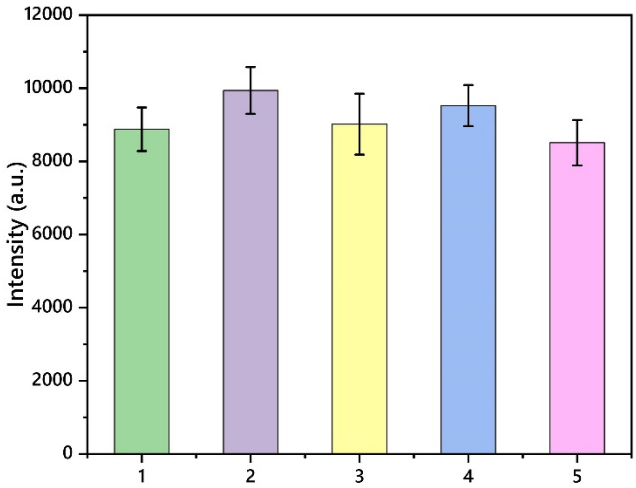

Figure S8. Intensity of the SERS spectrum of the 10^{-7} M R6G solution measured by five SERS sensors at the characteristic peak of 612 cm^{-1}.

The SERS spectra of different dye molecules are specific. We have calculated the Raman characteristic peaks and vibration properties of different dye molecules and compared them with the SERS spectra measured on the 3D Ag-AuNPs@NCF-based sensor, which verifies the accuracy of the spectra we obtained.

Table S3 Primary SERS peaks and corresponding vibration modes of CV, MG, SY, TZ and MO.

CV		**MG**	
SERS peak (cm^{-1})	**Vibration mode**	**SERS peak (cm^{-1})**	**Vibration mode**
1172	in-plane vibration of ring C–H	796	C-H out-of-plane ring bending
1394	symmetrical stretching of C–N, N-phenyl stretching	1172	C-H ring bending
1582	ring stretching of C–C	1396	N-phenyl stretching
1614	ring stretching of C–C	1618	C-C stretching
SY		**TZ**	
SERS peak (cm^{-1})	**Vibration mode**	**SERS peak (cm^{-1})**	**Vibration mode**
1053	C-S bending	1129	C-H deformation out-of-plane
1231	C-C in plane bending and C-N stretching vibration	1358	rocking of the phenyl ring and symmetric stretching of COO−
1499	C-H and N-H in-plane bending	1503	phenyl ring and C-C in plane bending
1599	C-C stretching vibration	1599	in-plane bending of OH and asymmetric stretching of COO−

MO	
SERS peak (cm^{-1})	**Vibration mode**
1117, 1193	Ph–N stretching
1131,1591	C–C stretching
1390	N=N group stretching

Table S4 Detection limit of CV, MG, SY, TZ and MO.

Type of dye	LOD (M)
CV	10^{-7}
MG	10^{-7}
SY	10^{-8}
TZ	10^{-8}
MO	10^{-7}

CNN model includes a convolution layer, a pooling layer, a full connection layer and an output layer. Its specific parameters are shown in the table below. The convolution layer is used for feature extraction of data. The pooling layer between different convolution layers can reduce the data dimension, so the number of parameters and the amount of calculation will decrease. The full connection layer is used to quantify the set of feature matrices. At the same time, in order to prevent over-fitting, we introduce a dropout layer with a coefficient of 0.5. Finally, the output layer predicts the category of input samples.

Table S5 Structure of the CNN model.

Layer type	**Parameters**
Convolutional	10 kernels of length 5, Relu activation.
Max pooling	Stride = 2
Convolutional	20 kernels of length 3, Relu activation.
Max pooling	Stride = 2
Convolutional	40 kernels of length 3, Relu activation.
View	-
Fully-connected	120 units, Relu activation
Dropout	Rate = 0.5
Fully-connected	84 units, Relu activation
Fully-connected	5 units (number of classes), Softmax activation